

INSULATED CYLINDRICAL ANTENNA IN A COLD MAGNETOPLASMA

A. V. Kudrin and E. Yu. Petrov

Department of Radiophysics
University of Nizhny Novgorod
23 Gagarin Ave., Nizhny Novgorod 603950, Russia

G. A. Kyriacou

Department of Electrical and Computer Engineering
Microwaves Laboratory
Democritus University of Thrace
Xanthi GR–67100, Greece

T. M. Zaboronkova

Department of Applied Physics
Technical University of Nizhny Novgorod
24 Minin St., Nizhny Novgorod 603950, Russia

Abstract—A study is made of the characteristics of a perfectly conducting cylindrical antenna insulated from the surrounding cold collisionless magnetoplasma by an isotropic coaxial cylindrical sheath for the case where the antenna is aligned with an external magnetic field and is excited by means of a delta-function voltage generator. A rigorous representation is obtained for the current distribution on an infinitely long antenna. It is shown that in the whistler frequency range, the current distribution of a sufficiently thin antenna is determined mainly by the eigenmode whose guided propagation is found to be supported along the antenna. Based on the results obtained for an infinitely long antenna, a generalized transmission-line theory is developed for determining the current distribution and the input impedance of an insulated antenna of finite length located in a resonant magnetoplasma. The influence of the sheath parameters on the antenna characteristics is analyzed.

1 Introduction

2 Formulation of the Problem for an Infinitely Long Antenna

3 Current Distribution on an Infinitely Long Antenna

- 3.1 Integral Representation of the Antenna Current
- 3.2 Eigenmodes Guided by a Thin Insulated Cylinder
- 3.3 Spectral Representation of the Antenna Current
- 3.4 Numerical Results for the Antenna Current

4 Current Distribution and Input Impedance of a Finite-Length Antenna

- 4.1 Current Distribution of a Finite-Length Antenna
- 4.2 Input Impedance of a Finite-Length Antenna

5 Conclusions

Acknowledgment

References

1. INTRODUCTION

The characteristics of cylindrical antennas in an unbounded cold magnetoplasma have been studied in a large number of papers. Many earlier works on this subject (see, e.g., [1–4] and references therein) treated the input impedance and the total field of a comparatively short dipole antenna with assumed current distribution. For the special case of a uniaxially anisotropic plasma medium, the problem of finding the current distribution and the input impedance of a cylindrical dipole antenna was considered exhaustively in [5–7]. The effect of the insulation of the antenna conducting surface from such a medium on the characteristics of an infinitely long cylindrical antenna was examined in [8].

When the surrounding medium is a magnetoplasma possessing gyrotropic properties, the problem of finding the current distribution on a cylindrical antenna becomes so complicated that there appear enormous difficulties for a solution. The complexity of this problem increases significantly for the case where a cold collisionless magnetoplasma is at resonance [6, 9]. Recall that the refractive index surface for one of the characteristic waves of a resonant magnetoplasma extends to infinity as the angle between the wavenormal direction and the gyroelectric axis of the medium approaches a certain value determined by the plasma parameters. For a nonresonant

magnetoplasma, the problem of the antenna current distribution is still tractable in some special cases [10, 11]. However, under resonance conditions, the conventional approaches such as that based on the integral-equation method cannot be employed readily for the antenna analysis. This is explained by the fact that, in contrast to the standard thin-antenna theory [12], it is now impossible to introduce the customary small parameter of antenna theory in the form of the ratio of the antenna-wire radius to the characteristic wavelength, since there always exist some wavenormal directions for which wavelengths in the plasma medium will be less than the wire cross-sectional extent. Therefore, most analyses of the cylindrical antenna in a resonant magnetoplasma use either the approximate transmission-line theory [13] or treat the current distribution on the antenna surface as a boundary-value problem [14–17].

Within the framework of the latter approach, as a first step, the current waves in an infinitely long antenna are determined. Then the truncation of the antenna to a finite length is performed, which leads to reflections of current waves of similar type from the antenna ends. Using such a waveguide approach, it was shown that, in general, the current on an uninsulated antenna immersed in a resonant magnetoplasma and excited by a voltage source comprises contributions from an eigen (bound) mode, which can exist in some frequency bands [18, 19], and from continuous-spectrum waves [14, 17]. In some cases important for applications, the eigenmode contribution is found to dominate the current distribution on a fairly thin antenna excited by a delta-function voltage source [17].

In recent years, there has been shown an increased interest in the characteristics of long cylindrical antennas insulated from the surrounding magnetoplasma by a concentric cylindrical sheath of a dielectric or free space. This interest has in particular been motivated by the results of experiments with a conducting ionospheric tether capable of guiding the current waves [20]. It should be noted that the insulation of the antenna from the surrounding magnetoplasma by a coaxial dielectric sheath can make the antenna characteristics less dependent on the plasma parameters and, hence, more predictable. Moreover, it is well known that the conducting wire immersed in the plasma is usually surrounded by the region of very reduced electron density formed around the antenna due to absorption of charged particles by the antenna surface. In theoretical considerations, the presence of this region known as the ion sheath can be taken into account in an idealized manner by considering the cylindrical antenna to be insulated from the surrounding plasma by a coaxial layer of free space.

In view of the above, the analysis of the insulated cylindrical antenna in a magnetoplasma is of crucial importance for an understanding of the behavior of the antenna characteristics under conditions of actual experiments. In the present paper, we consider a cylindrical antenna insulated from the surrounding magnetoplasma by a thin concentric dielectric or free-space sheath. The emphasis is placed on the case of a resonant magnetoplasma in which the refractive index surfaces may have unbounded branches. The main purpose of this work is to determine conditions under which the presence of the insulation can significantly affect the antenna characteristics.

We will first consider an infinitely long structure comprising the cylindrical conductor, the insulating sheath, and the plasma, assuming that this structure is aligned with an external magnetic field. Then we will proceed to the analysis of a more realistic finite cylindrical antenna.

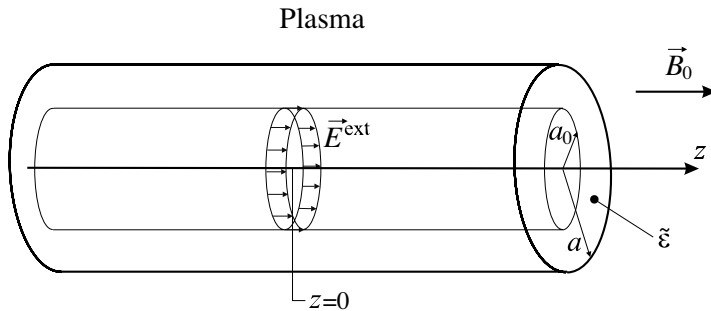


Figure 1. Geometry of the problem.

2. FORMULATION OF THE PROBLEM FOR AN INFINITELY LONG ANTENNA

The geometry of the problem for an antenna of infinite length is shown in Fig.1. A perfectly conducting cylinder of radius a_0 is oriented in such a way that its axis is aligned with a superimposed uniform static magnetic field $\vec{B}_0 = B_0 \hat{z}_0$ parallel to the z axis of a cylindrical coordinate system ρ , ϕ , and z . The antenna is insulated from the surrounding magnetoplasma by a homogeneous isotropic dielectric or free-space sheath which extends radially from $\rho = a_0$ to $\rho = a$. The plasma medium in the region $\rho > a$ is assumed cold, collisionless, and homogeneous. The antenna is driven at its center by a given time-harmonic voltage V applied uniformly around an infinitesimally thin

circumferential gap. This voltage creates the field

$$E_z^{\text{ext}} = V \delta(z) \quad (1)$$

on the cylinder surface, i.e., at $\rho = a_0 + 0$ (δ is a Dirac delta function). The time dependence for the generator (1) and all the field components is assumed as $\exp(i\omega t)$ and suppressed throughout the analysis.

The plasma medium is described by the relative dielectric tensor

$$\boldsymbol{\varepsilon} = \begin{pmatrix} \varepsilon & -ig & 0 \\ ig & \varepsilon & 0 \\ 0 & 0 & \eta \end{pmatrix} \quad (2)$$

whose elements can be found elsewhere (see, e.g., [21]). In what follows we focus on the case where $\text{sgn } \varepsilon \neq \text{sgn } \eta$. It is in this case that a magnetoplasma turns out to be resonant [6, 9, 22]. The insulating sheath around the antenna is characterized by the relative dielectric permittivity $\tilde{\varepsilon}$. If the medium inside the sheath is free space, then $\tilde{\varepsilon} = 1$.

The electric current \vec{J} induced on the antenna surface can be expressed in the form

$$\vec{J} = \hat{z}_0 I_z(z) \delta(\rho - a_0) + \hat{\phi}_0 I_\phi(z) \delta(\rho - a_0). \quad (3)$$

Here, I_z and I_ϕ are, respectively, the axial and azimuthal components of the surface-current density.

The time-harmonic Maxwell's equations inside the plasma ($\rho > a$) are given by

$$\nabla \times \vec{E} = -i\omega\mu_0\vec{H}, \quad (4)$$

$$\nabla \times \vec{H} = i\omega\epsilon_0 \boldsymbol{\varepsilon} \cdot \vec{E}, \quad (5)$$

where ϵ_0 and μ_0 are the permittivity and permeability of free space, respectively. Replacing the tensor $\boldsymbol{\varepsilon}$ in (5) by the scalar permittivity $\tilde{\varepsilon}$, we can obtain Maxwell's equations for the field inside the sheath ($a_0 < \rho < a$). The boundary conditions for the electric and magnetic fields are written as

$$E_z + E_z^{\text{ext}} = 0, \quad E_\phi = 0 \quad \text{at } \rho = a_0 + 0 \quad (6)$$

and

$$E_{\phi,z}(\rho = a - 0) = E_{\phi,z}(\rho = a + 0), \quad H_{\phi,z}(\rho = a - 0) = H_{\phi,z}(\rho = a + 0). \quad (7)$$

Solving the above Maxwell's equations with the boundary conditions (6) and (7), one can find the axial and azimuthal components of the current (3) induced on the antenna surface.

3. CURRENT DISTRIBUTION ON AN INFINITELY LONG ANTENNA

3.1. Integral Representation of the Antenna Current

The electric and magnetic fields in the regions $a_0 < \rho < a$ and $\rho > a$ can be expressed in the form of an integral representation by means of spatial Fourier transforms as follows:

$$\begin{aligned}\vec{E}(\rho, z) &= \frac{k_0}{2\pi} \int_{-\infty}^{\infty} \vec{E}(\rho, p) \exp(-ik_0pz) dp, \\ \vec{H}(\rho, z) &= \frac{k_0}{2\pi} \int_{-\infty}^{\infty} \vec{H}(\rho, p) \exp(-ik_0pz) dp,\end{aligned}\quad (8)$$

where p is the axial wavenumber normalized to the free-space wavenumber $k_0 = \omega(\epsilon_0\mu_0)^{1/2}$. In (8), use was made of the fact that all the field components are evidently independent of the azimuthal coordinate ϕ in the problem under consideration. The vector functions $\vec{E}(\rho, p)$ and $\vec{H}(\rho, p)$ can be described using two scalar functions $E_\phi(\rho, p)$ and $H_\phi(\rho, p)$. Inside the insulating layer ($a_0 < \rho < a$), they satisfy Bessel's equation

$$\hat{L} \begin{Bmatrix} E_\phi \\ H_\phi \end{Bmatrix} + k_0^2(\tilde{\epsilon} - p^2) \begin{Bmatrix} E_\phi \\ H_\phi \end{Bmatrix} = 0, \quad (9)$$

where

$$\hat{L} = \frac{\partial^2}{\partial \rho^2} + \frac{1}{\rho} \frac{\partial}{\partial \rho} - \frac{1}{\rho^2}.$$

Inside the plasma ($\rho > a$), the functions $E_\phi(\rho, p)$ and $H_\phi(\rho, p)$ satisfy the following system of second-order coupled differential equations [22]:

$$\begin{aligned}\hat{L}E_\phi + \frac{k_0^2}{\epsilon} [\epsilon(\epsilon - p^2) - g^2] E_\phi &= -ik_0^2 \frac{g}{\epsilon} pZ_0H_\phi, \\ \hat{L}H_\phi + k_0^2 \frac{\eta}{\epsilon} (\epsilon - p^2) H_\phi &= ik_0^2 \frac{\eta}{\epsilon} gpZ_0^{-1}E_\phi,\end{aligned}\quad (10)$$

where $Z_0 = (\mu_0/\epsilon_0)^{1/2} = 120\pi$ ohms is the impedance of free space. Equations (9) and (10) are easily derived from Maxwell's equations. The details of the derivation can be found in [22].

Solving the above field equations, we can write the tangential components (with respect to the surface $\rho = \text{const}$) of the electric and magnetic fields as follows [22]:

(i) inside the sheath ($a_0 < \rho < a$),

$$\begin{aligned} E_\phi(\rho, p) &= i [A_1 J_1(Q_0\rho/a_0) + A_2 Y_1(Q_0\rho/a_0)], \\ E_z(\rho, p) &= \frac{iQ_0}{k_0 a_0 \tilde{\varepsilon}} [B_1 J_0(Q_0\rho/a_0) + B_2 Y_0(Q_0\rho/a_0)], \\ H_\phi(\rho, p) &= -Z_0^{-1} [B_1 J_1(Q_0\rho/a_0) + B_2 Y_1(Q_0\rho/a_0)], \\ H_z(\rho, p) &= -Z_0^{-1} \frac{Q_0}{k_0 a_0} [A_1 J_0(Q_0\rho/a_0) + A_2 Y_0(Q_0\rho/a_0)]; \end{aligned} \quad (11)$$

(ii) inside the plasma ($\rho > a$),

$$\begin{aligned} E_\phi(\rho, p) &= i \sum_{k=1}^2 C_k H_1^{(2)}(Q_k\rho/a), \\ E_z(\rho, p) &= \frac{i}{k_0 a \eta} \sum_{k=1}^2 C_k n_k Q_k H_0^{(2)}(Q_k\rho/a), \\ H_\phi(\rho, p) &= -Z_0^{-1} \sum_{k=1}^2 C_k n_k H_1^{(2)}(Q_k\rho/a), \\ H_z(\rho, p) &= -Z_0^{-1} \frac{1}{k_0 a} \sum_{k=1}^2 C_k Q_k H_0^{(2)}(Q_k\rho/a). \end{aligned} \quad (12)$$

Here, J_m and Y_m are Bessel functions of the first and second kind of order m , respectively, $H_m^{(2)}$ are Hankel functions of the second kind of order m , and $A_{1,2}$, $B_{1,2}$, and $C_{1,2}$ are undetermined coefficients. The remaining notations are given by the expressions

$$\begin{aligned} Q_0 &= k_0 a_0 \tilde{q}(p), \quad Q_{1,2} = k_0 a q_{1,2}(p), \\ n_{1,2} &= -\varepsilon [p^2 + q_{1,2}^2(p) + (g^2 - \varepsilon^2)/\varepsilon] / (pg). \end{aligned} \quad (13)$$

The quantities \tilde{q} and $q_{1,2}$ are the normalized (to k_0) transverse wavenumbers referring to the insulating sheath and the magneto-plasma, respectively, and are described by the expressions

$$\tilde{q}(p) = (\tilde{\varepsilon} - p^2)^{1/2}, \quad (14)$$

$$q_k(p) = \left\{ \left[\varepsilon^2 - g^2 + \varepsilon\eta - (\eta + \varepsilon)p^2 + (-1)^k R_q(p) \right] / 2\varepsilon \right\}^{1/2}, \quad k=1, 2, \quad (15)$$

$$R_q(p) = -(\eta - \varepsilon) \left[(p^2 - P_b^2)^2 (p^2 - P_c^2) \right]^{1/2}, \quad (16)$$

where

$$P_{b,c} = \left\{ \varepsilon - (\eta + \varepsilon) \frac{g^2}{(\eta - \varepsilon)^2} + \frac{2\chi_{b,c}}{(\eta - \varepsilon)^2} \left[\varepsilon g^2 \eta (g^2 - (\eta - \varepsilon)^2) \right]^{1/2} \right\}^{1/2}, \quad (17)$$

with $\chi_b = -\chi_c = -1$. The square root in the expression (15) for $q_{1,2}$ is chosen to ensure the inequality $\text{Im } q_{1,2}(p) < 0$ appropriate to the radiation condition at infinity. It is worth noting that, in some frequency ranges, $\text{Im } q_{1,2}(p)$ may be zero in a cold collisionless magnetoplasma. In this case, it is necessary to introduce a small loss in the medium when choosing the branches of these functions. In the resulting formulas, however, we will pass to the case of a lossless plasma medium. The branches of the multivalued functions $\tilde{q}(p)$ and $R_q(p)$ may be chosen arbitrary. To avoid ambiguity, we will put $\text{Re } \tilde{q}(p) > 0$ and $\text{Re } R_q(p) > 0$ throughout.

By imposing the boundary conditions (6) and (7), we can determine the coefficients $A_{1,2}$, $B_{1,2}$, and $C_{1,2}$ in formulas (11) and (12). Then the axial and azimuthal components $I_z(p)$ and $I_\phi(p)$ of the Fourier-transformed surface-current density on the antenna can be obtained through the relations

$$I_z(p) = H_\phi(a_0, p), \quad I_\phi(p) = -H_z(a_0, p). \quad (18)$$

Evaluating $H_\phi(\rho, p)$ and $H_z(\rho, p)$ at $\rho = a_0$ and substituting them into (18), after some lengthy algebra we arrive at

$$I_z(z) = -\frac{i}{2\pi} \frac{V}{Z_0} k_0^2 a_0 \tilde{\varepsilon} \int_{-\infty}^{\infty} \frac{F_z(p)}{\Lambda(p)} \exp(-ik_0 p z) dp, \quad (19)$$

$$I_\phi(z) = \frac{2i}{\pi^3} \frac{V}{Z_0} k_0 \tilde{\varepsilon} \int_{-\infty}^{\infty} \frac{F_\phi(p)}{\Lambda(p)} \exp(-ik_0 p z) dp, \quad (20)$$

where

$$\begin{aligned} F_z(p) &= S_{10}^2 D_{00} + S_{10} S_{11} (D_{01} + D_{10}) + S_{11}^2 D_{11}, \\ F_\phi(p) &= Q_1 H_0^{(2)}(Q_1) H_1^{(2)}(Q_2) - Q_2 H_0^{(2)}(Q_2) H_1^{(2)}(Q_1), \\ \Lambda(p) &= Q_0 [S_{00}(S_{10} D_{00} + S_{11} D_{01}) + S_{01}(S_{10} D_{10} + S_{11} D_{11})], \\ D_{00} &= Q^2 H_1^{(2)}(Q_1) H_1^{(2)}(Q_2) (n_1 - n_2), \\ D_{01} &= Q \left[n_2 Q_1 H_0^{(2)}(Q_1) H_1^{(2)}(Q_2) - n_1 Q_2 H_0^{(2)}(Q_2) H_1^{(2)}(Q_1) \right], \\ D_{10} &= -Q \frac{\tilde{\varepsilon}}{\eta} \left[n_1 Q_1 H_0^{(2)}(Q_1) H_1^{(2)}(Q_2) - n_2 Q_2 H_0^{(2)}(Q_2) H_1^{(2)}(Q_1) \right], \\ D_{11} &= \frac{\tilde{\varepsilon}}{\eta} Q_1 Q_2 H_0^{(2)}(Q_1) H_0^{(2)}(Q_2) (n_1 - n_2), \end{aligned}$$

$$S_{lm} = J_l(Q_0)Y_m(Q) - J_m(Q)Y_l(Q_0), \quad Q = k_0 a \tilde{q}(p), \quad l=0, 1, \quad m=0, 1. \quad (21)$$

Formulas (19)–(21) constitute the solution to the problem of the current distribution on the surface of an infinite, perfectly conducting insulated cylinder and are valid for a magnetoplasma described by the dielectric tensor of general form (2).

The expression $\Lambda(p)$ in (19) and (20) has a clear physical meaning. It is not difficult to verify that the relation

$$\Lambda(p) = 0 \quad (22)$$

is the dispersion equation for axisymmetric eigenmodes guided by a perfectly conducting insulated cylinder in a magnetoplasma. Further analysis of the current distribution on the cylinder surface is preceded by solving the dispersion equation for the cases of interest to us.

3.2. Eigenmodes Guided by a Thin Insulated Cylinder

We now consider eigenmodes which can be guided by an insulated cylinder. The propagation constants (axial wavenumbers) of these modes are poles of the integrands in formulas (19) and (20). As mentioned above, these poles are zeros of $\Lambda(p)$. Although the branch points $p = \pm P_{b,c}$ of the functions $q_k(p)$ and $R_q(p)$ are also roots of (22), they are not poles of the above-mentioned integrands since both the numerators and denominators of the integrands vanish at these points so that the integrands approach finite values. As a result, the integrands remain finite at the points $p = \pm P_{b,c}$. Furthermore, it can be shown that the branch points $p = \pm \tilde{\varepsilon}^{1/2}$ of the function $\tilde{q}(p)$ are not poles of the integrands in (19) and (20). Recall that a perfectly conducting sheathless cylinder immersed in a resonant magnetoplasma can in general support a single axisymmetric eigenmode if $\varepsilon > 0$ and $\eta < 0$ [14, 17, 19]. In what follows we limit ourselves to consideration only of the whistler frequency range. The resonant part of the whistler range includes the subranges

$$\omega_{LH} < \omega < \omega_H/2 < \omega_p, \quad (23)$$

$$\omega_H/2 < \omega < \omega_H < \omega_p, \quad (24)$$

where ω_{LH} is the lower hybrid frequency and ω_H and ω_p are the gyrofrequency and the plasma frequency of electrons, respectively. We note that waves whose frequencies lie in intervals (23) and (24), in which $\varepsilon > 0$, $g < 0$, and $\eta < 0$, are of great importance for numerous promising applications (see, e.g., [20, 22]). As is known,

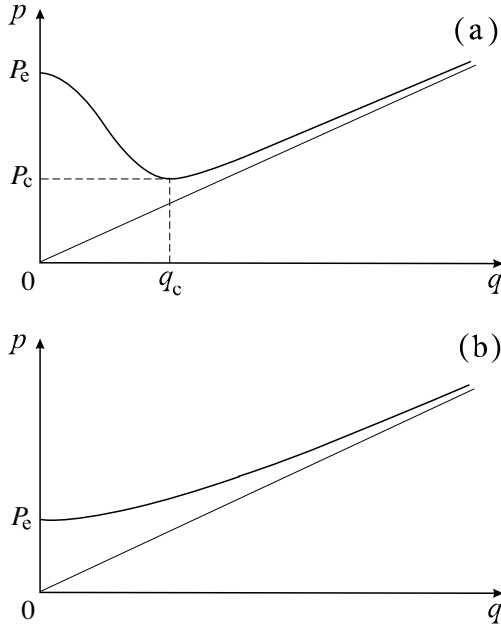


Figure 2. Typical whistler-mode refractive index surfaces for (a) frequency range (23) and (b) frequency range (24).

only one characteristic wave of a cold homogeneous magnetoplasma is propagating in the whistler range. This wave is commonly called the whistler mode. The other characteristic wave is evanescent in the frequency range considered. As an example, Figs. 2a and 2b show typical whistler-mode refractive index surfaces for frequency ranges (23) and (24). The refractive-index surface for range (23) is described by the function $q_1(p)$ in the region $0 < q < q_c$, and by the function $q_2(p)$ in the region $q_c < q < \infty$, where the point $q_c = q_1(P_c) = q_2(P_c)$ corresponds to conical-refraction whistler-mode waves possessing the axial wavenumber $p = P_c$ [22]. The refractive-index surface for range (24) is described by the function $q_2(p)$. It is worth mentioning that the quantity $q_1(p)$ cannot be purely real for all real values of p at frequencies (24). We also introduce a quantity $P_e = (\varepsilon - g)^{1/2}$, which is the axial wavenumber of a whistler-mode wave propagating in a homogeneous unbounded magnetoplasma strictly along the external magnetic field (see Figs. 2a and 2b). At $p = P_e$, we evidently have $q_1(P_e) = 0$ for range (23) and $q_2(P_e) = 0$ for range (24).

The properties of the eigenmode guided by a sheathless cylinder in a magnetoplasma at frequencies (23) and (24) were considered in

detail in [17]. It was shown that the propagation constant $p = p_0$ of the eigenmode can be found by solving the equation

$$n_1 Q_1 H_0^{(2)}(Q_1) H_1^{(2)}(Q_2) - n_2 Q_2 H_0^{(2)}(Q_2) H_1^{(2)}(Q_1) = 0, \quad (25)$$

which follows from equation (22) in the case where $a_0 = a$. In the frequency range (23), the propagation constant p_0 is found to lie in the region

$$P_b < p_0 < P_c, \quad (26)$$

In this case, $q_1(p_0)$ and $q_2(p_0)$ are complex and satisfy the relationship $q_1(p_0) = -q_2^*(p_0)$, where the asterisk stands for complex conjugate. Note that the mode field is transversely decaying since $\text{Im } q_{1,2}(p) < 0$. In the frequency range (24), inequalities (26) hold if the frequency ω is not well away from half the electron gyrofrequency. With increasing ω , the propagation constant p_0 goes from the region (26) to the region

$$P_c < p_0 < P_e, \quad (27)$$

in which q_1 and q_2 are both purely imaginary. It is worth recalling that the solution of equation (25) can be approximated by

$$p_0 = \varepsilon^{1/2} \quad (28)$$

in the limiting case $a_0 \rightarrow 0$, and by

$$p_0 = \{\varepsilon + [g^2 \varepsilon / (\varepsilon - \eta)]^{1/2}\}^{1/2} \quad (29)$$

in the limiting case $a_0 \rightarrow \infty$ [17].

It should be emphasized that the eigenmode guided by a perfectly conducting sheathless cylinder can exist only in the case of a gyrotropic plasma. The fact that the off-diagonal term g of the plasma dielectric tensor does not enter formula (28) requires explanation. For nonzero a_0 , it can be shown that the element g does enter the solution of the dispersion equation (25). However, in the limiting case $a_0 \rightarrow 0$, the terms in the rigorous expression of the solution, which comprise the element g , become small in comparison with $\varepsilon^{1/2}$. These terms were therefore neglected when reducing the solution to the approximate form (28).

In the presence of the insulation, new eigenmodes can appear. For most applications, however, the thickness $\Delta a = a - a_0$ of the insulating layer is rather small such that $k_0 \Delta a \tilde{\varepsilon}^{1/2} \ll 1$, and only a single eigenmode can be found to exist, as in the case of a sheathless cylinder. Let us show that the characteristics of the eigenmode can be affected significantly by the insulating sheath. Equation (22),

which defines the propagation constant of this eigenmode, is fairly complicated to be solved analytically in the general case. However, the limiting case where $s = (a - a_0)/a_0 \ll 1$ and $\kappa = k_0 a_0 \ll 1$ allows some analytical treatment. To do this, we will also assume that the inequalities $k_0 a |\tilde{q}(p)| \ll 1$ and $k_0 a |q_{1,2}(p)| \ll 1$ hold for $p < P_c$. Making use of the identity [23]

$$J_1(\zeta) Y_0(\zeta) - J_0(\zeta) Y_1(\zeta) = 2/\pi\zeta,$$

we replace the cylindrical functions entering the expression for $\Lambda(p)$ in (22) by their small-argument approximations. It can be shown in this case that

$$\begin{aligned} S_{00} &= \frac{2}{\pi} s + O(s^2), & S_{01} &= \frac{2}{\pi\kappa\tilde{q}} \left[1 - s + O(s^2) \right], \\ S_{10} &= \frac{2}{\pi\kappa\tilde{q}} \left[1 + O(s^2) \right], & S_{11} &= \frac{2}{\pi} s + O(s^2). \end{aligned} \quad (30)$$

Assuming, in addition, that $|\ln \kappa| \gg 1$ and $|\ln k_0 a| \gg |\ln q_k(p)|$ and neglecting small terms of order $\kappa \ln^2 \kappa$ and of order s^2 in the expression for $\Lambda(p)$, after some algebra we obtain

$$p_0 = \varepsilon^{1/2} \left[1 - s \left(1 + \frac{1}{\ln \kappa} \right) \right]^{1/2} \left[1 - s \left(1 + \frac{\varepsilon}{\tilde{\varepsilon} \ln \kappa} \right) \right]^{-1/2}. \quad (31)$$

For zero thickness of the insulating sheath when $s = 0$, formula (31) yields the result given by (28).

Note that the quantity p_0 determined by (31) lies in the same intervals as for the case of a sheathless antenna where $s = 0$. Consequently, for large ρ , the mode field decays exponentially in the radial direction with distance from the boundary $\rho = a$ of the insulating sheath.

The behavior of the propagation constant p_0 as a function of the normalized thickness s of the insulation was analyzed by numerically solving the rigorous dispersion equation (22) for the case $\tilde{\varepsilon} = 1$, which simulates the presence of the ion sheath around the conducting cylinder. The elements of the dielectric tensor (2) at frequencies (23) and (24) may be written approximately as [21, 22]

$$\varepsilon = \left[1 + X_p / (Y^2 - 1) \right] (1 - Y_{\text{LH}}^2), \quad (32)$$

$$g = -X_p Y / (Y^2 - 1), \quad (33)$$

$$\eta = 1 - X_p, \quad (34)$$

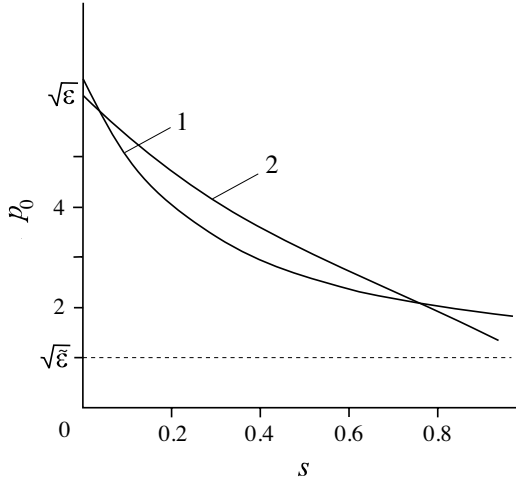


Figure 3. Eigenmode propagation constant p_0 as a function of $s = (a - a_0)/a_0$ for $\tilde{\epsilon} = 1$, $X_p = 9 \times 10^4$, $Y = 46.6$, $Y_{LH} = 0.26$, and $\kappa = 6.28 \times 10^{-6}$. Curves 1 and 2 represent the results of the numerical solution of the rigorous dispersion equation (22) and the approximate solution given by formula (31), respectively.

where $X_p = \omega_p^2/\omega^2$, $Y = \omega_H/\omega$, and $Y_{LH} = \omega_{LH}/\omega$. For numerical calculations, we took the following values of the plasma parameters and the quantity κ : $X_p = 9 \times 10^4$, $Y = 46.6$, $Y_{LH} = 0.26$, and $\kappa = 6.28 \times 10^{-6}$ ($\ln \kappa = -12$). Note that the chosen values of X_p , Y , Y_{LH} , and $\ln \kappa$ are typical of experiments on the excitation of whistlers in the Earth's ionosphere and the laboratory plasma. The values of p_0 , obtained from (22) and (31), are shown in Fig. 3. It is seen in Fig. 3 that formula (31) yields a reasonably good approximation to the exact p_0 even when s is of order unity. It is to be noted that p_0 decreases monotonically to $\tilde{\epsilon}^{1/2}$ with increasing s . For a sheathless antenna, the rigorous solution for p_0 (see curve 1 in Fig. 3) exceeds only slightly the approximate solution (28) obtained on the assumption that $s = 0$. The most important conclusion which may be drawn from the results shown in Fig. 3 is that the presence of a sufficiently thin sheath around the antenna wire can significantly affect the value of the eigenmode propagation constant. Moreover, the value of s , required to cause a significant change in p_0 as compared with the propagation constant in the case of a sheathless cylinder, is smaller, the higher the tensor element $\tilde{\epsilon}$.

It should be noted that the waves guided along a perfectly

conducting insulated cylinder immersed in a magnetoplasma have previously been discussed in [24] for the case where the axis of the cylinder is parallel to the direction of the external magnetic field. In [24], the exact dispersion equation, obtained with the help of Maxwell's equations and the boundary conditions, has been reduced to the approximate form in which the contribution of the terms comprising one of the transverse wavenumbers $q_{1,2}$ is neglected. The approximation used in [24] can be employed in the case $p \gg P_e$ (see [22] for details). However, as follows from the above-presented results, the propagation constants of true eigenmodes guided by the cylinder in the whistler range should lie in regions (26) or (27). In those regions, both branches q_1 and q_2 of the transverse wavenumber must be taken into account in the dispersion equation in order to obtain the propagation constant p_0 properly. Therefore, the expressions derived in [24] do not give the correct value for p_0 in the whistler range. This becomes fairly evident when one tries to perform the limiting transition from the expressions given in [24] to the solution for the propagation constant of the eigenmode in the case where the sheath thickness vanishes.

3.3. Spectral Representation of the Antenna Current

To obtain a representation which exhibits the eigenmode contribution to the total current explicitly, it is necessary to make a suitable deformation of the integration path in the complex p plane in formulas (19) and (20). We will consider this procedure in detail for the frequency range (23). Before proceeding in this way, we analyze the analytic properties of the integrands entering expressions (19) and (20) and comprising multivalued functions $\tilde{q}(p)$, $R_q(p)$, and $q_{1,2}(p)$. It can be shown with the help of the identities [23]

$$J_n(\zeta e^{i\pi}) = e^{in\pi} J_n(\zeta), \quad Y_n(\zeta e^{i\pi}) = e^{-in\pi} Y_n(\zeta) + 2i \cos n\pi J_n(\zeta)$$

that the integrands of (19) and (20) are independent of the sign of $\tilde{q}(p)$, so that $p = \pm\tilde{\varepsilon}^{1/2}$ are not their branch points. Moreover, these integrands are invariant with respect to the replacement $q_1 \leftrightarrow q_2$. Hence, the branch cuts starting at the points $p = \pm P_{b,c}$ and going along the lines $\text{Re } R_q = 0$ need not be taken into account (see [22] for details). Thus, the singularities present are the poles $p = \pm p_0$ due to zeros of $\Lambda(p)$ and the branch cuts going along the lines $\text{Im } q_{1,2} = 0$ and associated with the branch points $p = \pm P_e = \pm(\varepsilon - g)^{1/2}$ and $p = \pm P_o = \mp i(-\varepsilon - g)^{1/2}$ at which $q_1(\pm P_e) = 0$ and $q_2(\pm P_o) = 0$.

The sheet of Riemann surface of the analyzed integrands, which corresponds to the condition $\text{Im } q_{1,2} < 0$ stipulated above, is shown in

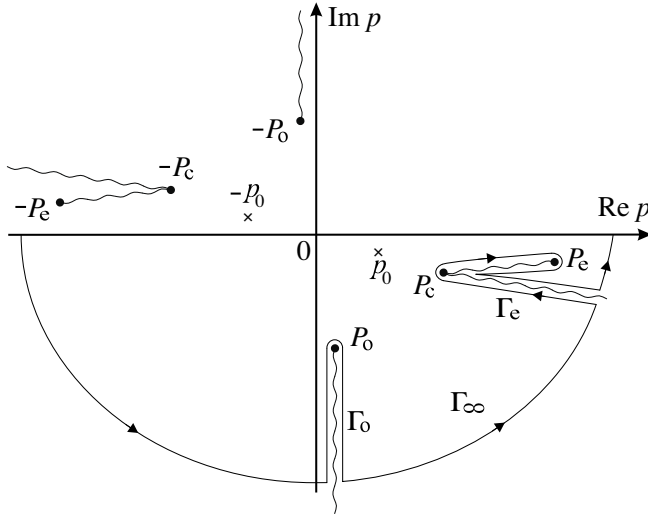


Figure 4. Integration contours in the complex p plane for frequency range (23).

Fig. 4 for range (23). In this figure, the branch cuts connecting the branch points $p = P_c$ and $p = P_e$ as well as $p = -P_c$ and $p = -P_e$ go along the lines at which $\text{Im } q_1 = 0$. Other branch cuts go along the lines at which $\text{Im } q_2 = 0$. Also shown are the poles $p = \pm p_0$. If the plasma medium is lossless, then the propagation constants $p = \pm p_0$ are real and are located on the real p axis. Also, the branch cuts tend to merge with either real or imaginary p axis in this case. To avoid ambiguity in the mutual location of these singularities, Fig. 4 was plotted for the case where small losses are introduced. Then the poles and the branch cuts are slightly displaced off the corresponding axes, as shown in Fig. 4.

We now separate explicitly the contribution of the eigenmode to the general integral representation of the antenna current. The axial distribution of the total current $I(z) = 2\pi a_0 I_z(z)$ through the cylinder cross section is considered in detail. For definiteness, we will discuss the current for positive z . The case of negative z can be considered analogously. Let us use the integration contour $\Gamma_\infty + \Gamma_0 + \Gamma_e$ in (19). This contour is shown in Fig. 4. Since the integral over the semicircle Γ_∞ of infinite radius is zero, the current $I(z)$ is determined only by the residue of the pole $p = p_0$ and the integrals around the branch cuts, i.e., along the contours Γ_0 and Γ_e . As a result, we arrive at the

following expression of the current for $z > 0$:

$$I(z) = \alpha_0 \exp(-ik_0 p_0 z) + \Delta I(z) \quad (35)$$

where

$$\alpha_0 = -\frac{V}{Z_0} 2\pi(k_0 a_0)^2 \tilde{\varepsilon} F_z(p) \left[\frac{d\Lambda}{dp} \right]^{-1} \Big|_{p=p_0}, \quad (36)$$

$$\Delta I(z) = \int_{\Gamma_o} \mathcal{I}(p) \exp(-ik_0 p z) dp + \int_{\Gamma_e} \mathcal{I}(p) \exp(-ik_0 p z) dp, \quad (37)$$

with

$$\mathcal{I}(p) = -i \frac{V}{Z_0} (k_0 a_0)^2 \tilde{\varepsilon} \frac{F_z(p)}{\Lambda(p)}. \quad (38)$$

The first term on the right-hand side of (35) represents the eigenmode contribution to the total current $I(z)$. The quantity α_0 is the amplitude coefficient of the eigenmode current. The term $\Delta I(z)$ gives the contribution of continuous-spectrum waves to the total current. Note that the circumferential current $I_\phi(z)$ can be represented in a similar manner:

$$I_\phi(z) = \beta_0 \exp(-ik_0 p_0 z) + \Delta I_\phi(z), \quad (39)$$

where β_0 is the amplitude coefficient of the eigenmode contribution and $\Delta I_\phi(z)$ is the contribution of continuous-spectrum waves to $I_\phi(z)$. We do not give here formulas for β_0 and $\Delta I_\phi(z)$ for the sake of brevity.

It may be noted that the above-described transformation of integration path yields the so-called spectral representation for the antenna current [22]. In such a representation, the contribution due to the eigenmode belonging to the discrete spectrum is expressed by a separate term, whereas the contribution due to waves of the continuous spectrum is described by integrals along paths at which one of the transverse wavenumbers is purely real. At large distances z from the excitation point of the antenna, the integrals along the contours Γ_o and Γ_e can be evaluated by using the steepest-descent method in a manner similar to the treatment of a sheathless antenna in [17]. We will not dwell on the corresponding analytical calculations and immediately proceed to discussing the numerical results for the current distribution.

3.4. Numerical Results for the Antenna Current

Numerical calculations performed under the same conditions that were used for the derivation of (31) show that the inequality $|I| \gg 2\pi a_0 |I_\phi|$ holds with a sufficient margin. Moreover, the antenna current is almost entirely determined by the eigenmode contribution. This

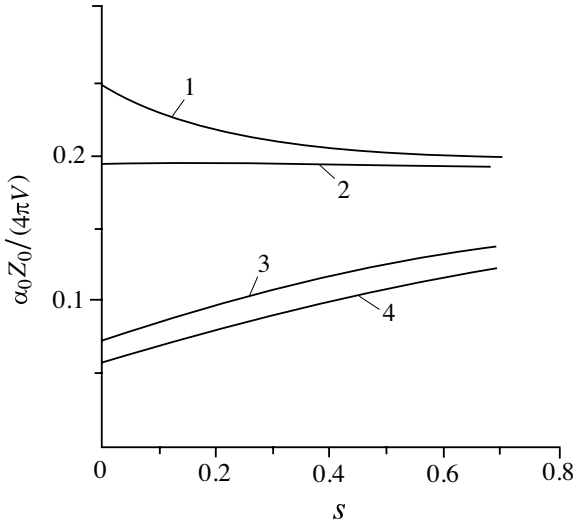


Figure 5. Normalized amplitude α_0 as a function of s for $\tilde{\epsilon} = 1$, $k_0 a_0 Y = 2.9 \times 10^{-4}$, and different plasma parameters: $X_p = 9 \times 10^4$, $Y = 46.6$, and $Y_{LH} = 0.26$ (curve 1); $X_p = 5.6 \times 10^5$, $Y = 116.5$, and $Y_{LH} = 0.65$ (curve 2); $X_p = 9 \times 10^3$, $Y = 46.6$, and $Y_{LH} = 0.26$ (curve 3); and $X_p = 5.6 \times 10^4$, $Y = 116.5$, and $Y_{LH} = 0.65$ (curve 4).

contribution is illustrated by Fig. 5 showing the amplitude α_0 as a function of the normalized sheath thickness $s = (a - a_0)/a_0$ for $\tilde{\epsilon} = 1$, $k_0 a_0 Y = 2.9 \times 10^{-4}$, and different values of the plasma parameters. For comparison, Fig. 6 shows the normalized amplitude β_0 of the eigenmode contribution to the azimuthal component of the surface-current density. This figure is plotted for the same parameter values as in Fig. 5. It is worth mentioning that the plasma parameters are chosen such that, in Figs. 5 and 6, curves 1 and 2 correspond to one value of the ratio ω_p/ω_H , while curves 3 and 4 correspond to another value of this ratio. It follows from Figs. 5 and 6 that $|\beta_0| \ll |\alpha_0|/(2\pi a_0)$ for the chosen parameter values. Moreover, the quantity β_0 rapidly decreases with s .

It is seen in Figs. 5 and 6 that the quantities α_0 and β_0 increase significantly with increasing plasma density if the insulating layer is not too thick ($s < 0.5$). This is explained by the fact that, in this case, the eigenmode field turns out to be more localized for a higher plasma density. We do not present plots with the field structure of this mode since they are similar to those for a sheathless antenna (see [17] for details). The only difference can be observed for the field inside the sheath region in which the components E_ρ and $H_{\phi,z}$

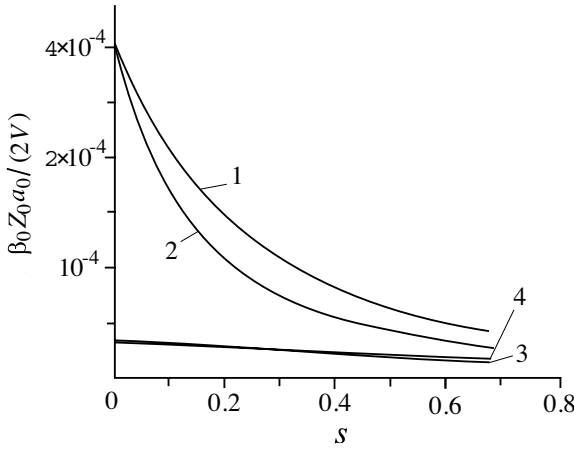


Figure 6. Normalized amplitude β_0 as a function of s for $\tilde{\varepsilon} = 1$, $k_0 a_0 Y = 2.9 \times 10^{-4}$, and different plasma parameters. Curves 1–4 are plotted for the same values of X_p , Y , and Y_{LH} as the corresponding curves in Fig. 5.

decay approximately as ρ^{-1} , whereas the components $E_{\phi,z}$ and H_ρ increase almost linearly with ρ . Despite the fact that the eigenmode is hybrid, the components E_ρ and H_ϕ predominate in the field structure. Thus the eigenmode has quasi-TEM behavior. For a thicker insulation ($s > 0.5$), the quantities α_0 and β_0 are affected only slightly by the parameters of the surrounding plasma. In this case, almost all of the power carried by the eigenmode is confined to the sheath region and the field structure in the vicinity of the antenna wire becomes much closer to that of a TEM wave.

The contribution of the continuous-spectrum waves to the current $I(z)$ is shown in Fig. 7 obtained numerically for different values of s . The computations were performed for the same parameter values as for Fig. 3. It is evident from the dependences presented that the contribution of continuous-spectrum waves to the current distribution is negligible at large and moderate values of z , so that the function $I(z)$ is determined mainly by the eigenmode guided by the cylinder. As z decreases, the relative contribution of continuous-spectrum waves to the antenna current increases and becomes dominant at the sufficiently small values of z ($z < a_0(-\eta/\varepsilon)^{1/2}$). Finally, at $z = 0$, the current goes to infinity. This is related to the fact that a delta function was used to represent the z dependence of E_z^{ext} . The singularity in the current distribution disappears if the voltage is applied to a region of finite length along the z axis. Indeed, if the antenna is excited by a voltage

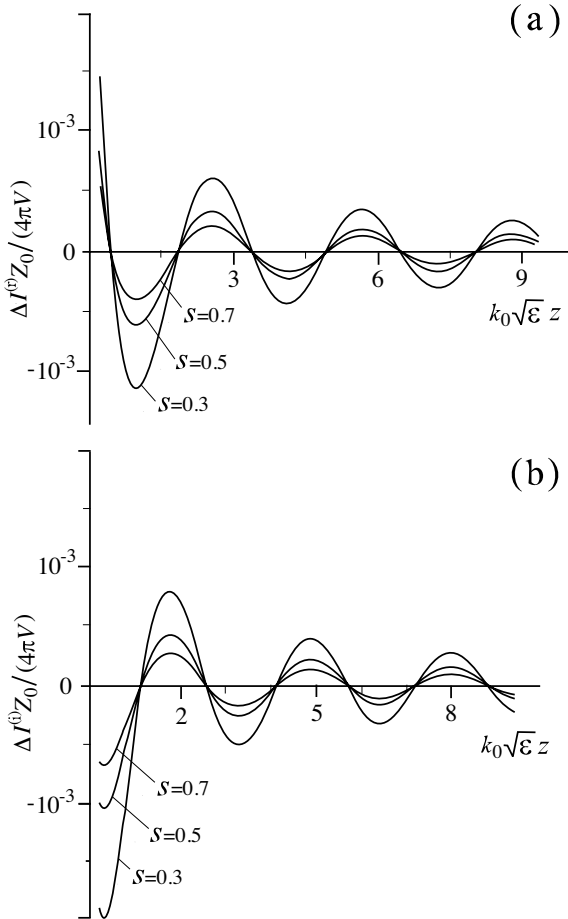


Figure 7. Distributions of $\Delta I^{(r)}(z) = \text{Re} \Delta I(z)$ and $\Delta I^{(i)}(z) = \text{Im} \Delta I(z)$ along an infinite antenna for various values of s and the same parameter values as for Fig. 3.

applied to a narrow gap of width $2d$ so that

$$E_z^{\text{ext}} = \begin{cases} V/(2d) & \text{for } |z| < d, \\ 0 & \text{for } |z| > d, \end{cases}$$

then a factor $\sin(k_0pd)/(k_0pd)$ should be inserted in the integrands of (19) and (20). With this factor, the corresponding integrals are convergent at $z = 0$, and the singularity in the current distribution does not appear. Moreover, it can be shown that, for a reasonable gap width such that $2d > a_0$, the current is determined by the eigenmode on the

whole antenna surface. Since the inequality $|\Delta I_\phi(z)| \ll |\Delta I(z)|/(2\pi a_0)$ holds in the case considered, plots for the quantity $\Delta I_\phi(z)$ are not given here.

Summarizing the main results following from the above analysis, we can state that (i) the total current $I(z)$ through the cross section of a thin insulated cylindrical antenna of infinite length is determined by the eigenmode whose propagation constant can be found by solving the dispersion equation (22), (ii) the eigenmode amplitude depends noticeably on s , and (iii) the continuous-spectrum contribution to the total current decreases rather rapidly with increasing thickness of the insulating sheath and is significantly smaller than that for a sheathless antenna. At the same time, the eigenmode wavelength $\lambda = 2\pi/(k_0 p_0)$ depends significantly on s (see Fig. 3), while the ‘‘period’’ of oscillations of the continuous-spectrum current is almost independent of s and turns out to be rather close to $\lambda_c = 2\pi/(k_0 P_c)$. It is interesting to note that if $\omega_p \gg \omega_H$ and $\omega \gg \omega_{LH}$, in which case formulas (32) and (34) are simplified to $\varepsilon = X_p/(Y^2 - 1)$ and $\eta = -X_p$, then the expression (17) for P_c reduces to $P_c = 2X_p^{1/2}/Y = 2\omega_p/\omega_H$ and, hence, $\lambda_c = \pi\omega_H/(k_0\omega_p)$. Another important conclusion is that the circumferential current of a thin cylindrical antenna in a magnetoplasma is negligibly small compared with the axial current, regardless of the thickness of the insulation.

To conclude this section, we note that although the above results are obtained for the case of an unbounded plasma medium located in the region $a < \rho < \infty$, they can be extended to an insulated antenna surrounded by a plasma layer of finite thickness. Let us assume that the plasma is located in the region $a < \rho < b$ and an outer region $\rho > b$ is free space, which is typical of many laboratory experiments. It is evident that the results of the foregoing analysis corresponding to the limit $b \rightarrow \infty$ continue to hold in the case where b is finite if the spatial scale of decay of the dominant eigenmode in the $\hat{\rho}_0$ direction inside the plasma layer is much smaller than the layer thickness $b - a$. That is,

$$b - a \gg (k_0 |\text{Im } q_{1,2}(p_0)|)^{-1}.$$

In the presence of the ion sheath around the antenna wire, a is of the order of the Debye length, which must be much smaller than b in order for a mixture of charged particles in the region between $\rho = a$ and $\rho = b$ to be a plasma. Then the above inequality is rewritten as $b \gg (k_0 |\text{Im } q_{1,2}(p_0)|)^{-1}$.

4. CURRENT DISTRIBUTION AND INPUT IMPEDANCE OF A FINITE-LENGTH ANTENNA

4.1. Current Distribution of a Finite-Length Antenna

Taking into account the dominant contribution of the eigenmode to the total current, we can determine approximately the current distribution of a finite-length antenna with the help of the concept of reflections of the current eigenmode from the antenna ends.

Note that in the case of antenna excitation by a delta-function voltage at $z = 0$, the components of the eigenmode field for an infinite antenna are expressed as

$$\begin{aligned} E_\phi(\rho, z) &= \operatorname{sgn}(z) \mathcal{E}_0 \mathcal{E}_\phi(\rho, p_0) \exp(-ik_0 p_0 |z|), \\ E_z(\rho, z) &= \mathcal{E}_0 \mathcal{E}_z(\rho, p_0) \exp(-ik_0 p_0 |z|), \\ H_\phi(\rho, z) &= \mathcal{E}_0 \mathcal{H}_\phi(\rho, p_0) \exp(-ik_0 p_0 |z|), \\ H_z(\rho, z) &= \operatorname{sgn}(z) \mathcal{E}_0 \mathcal{H}_z(\rho, p_0) \exp(-ik_0 p_0 |z|), \end{aligned} \quad (40)$$

where \mathcal{E}_0 is a certain amplitude factor, and $\mathcal{E}_{\phi,z}(\rho, p_0)$ and $\mathcal{H}_{\phi,z}(\rho, p_0)$ are functions describing the dependence of the azimuthal and axial components of the eigenmode field on the radial cylindrical coordinate ρ . Representation (40) is readily obtained from (8) by evaluation of the residue of the eigenmode pole $p = p_0$ enclosed by the integration contour shown in Fig. 4. It may be adopted without any loss of generality that the functions $\mathcal{E}_{\phi,z}(\rho, p_0)$ and $\mathcal{H}_{\phi,z}(\rho, p_0)$ satisfy the following relationships [22]:

$$\begin{aligned} \mathcal{E}_\phi(\rho, p_0) &= -\mathcal{E}_\phi(\rho, -p_0), & \mathcal{E}_z(\rho, p_0) &= \mathcal{E}_z(\rho, -p_0), \\ \mathcal{H}_\phi(\rho, p_0) &= \mathcal{H}_\phi(\rho, -p_0), & \mathcal{H}_z(\rho, p_0) &= -\mathcal{H}_z(\rho, -p_0). \end{aligned} \quad (41)$$

These relationships will be used in what follows.

An antenna of length $2L$ can be described as a single-wire transmission line consisting of the conducting cylinder, the dielectric sheath, and the surrounding plasma. The azimuthal component of the magnetic field inside the sheath is then represented approximately as

$$H_\phi(\rho, z) = \mathcal{E}_0 \mathcal{H}_\phi(\rho, p_0) \left\{ e^{-ik_0 p_0 |z|} + R_1 e^{-ik_0 p_0 z} + R_2 e^{ik_0 p_0 z} \right\}, \quad |z| < L, \quad (42)$$

where R_1 and R_2 are coefficients which can be determined from conditions for the current at the antenna ends. To find R_1 and R_2 , we apply the conditions

$$I(z = \pm L) = 2\pi a_0 H_\phi(a_0, z = \pm L) = 0 \quad (43)$$

for the axial current at $z = \pm L$. Using (43), one obtains

$$R_1 = R_2 = -\frac{1}{2 \cos(k_0 p_0 L)} \exp(-ik_0 p_0 L) \quad (44)$$

and

$$H_\phi(\rho, z) = \mathcal{E}_0 \mathcal{H}_\phi(\rho, p_0) \frac{i}{\cos(k_0 p_0 L)} \sin[k_0 p_0(L - |z|)], \quad |z| < L. \quad (45)$$

The field E_z can be obtained by making the replacements $H_\phi(\rho, z) \rightarrow E_z(\rho, z)$ and $\mathcal{H}_\phi(\rho, p_0) \rightarrow \mathcal{E}_z(\rho, p_0)$ in (42) and using formula (44). The result is

$$E_z(\rho, z) = \mathcal{E}_0 \mathcal{E}_z(\rho, p_0) \frac{i}{\cos(k_0 p_0 L)} \sin[k_0 p_0(L - |z|)], \quad |z| < L. \quad (46)$$

In deriving formulas (45) and (46), use was made of the fact that $\mathcal{H}_\phi(\rho, p_0)$ and $\mathcal{E}_z(\rho, p_0)$ are even functions of the propagation constant (see (41)). In order to obtain the components H_z and E_ϕ , one should bear in mind that the corresponding quantities $\mathcal{H}_z(\rho, p_0)$ and $\mathcal{E}_\phi(\rho, p_0)$ are odd functions of the propagation constant. Thus,

$$H_z(\rho, z) = \mathcal{E}_0 \mathcal{H}_z(\rho, p_0) \left\{ \operatorname{sgn}(z) e^{-ik_0 p_0 |z|} + R_1 e^{-ik_0 p_0 z} - R_2 e^{ik_0 p_0 z} \right\}, \quad |z| < L. \quad (47)$$

Substituting for $R_{1,2}$ from (44) yields

$$H_z(\rho, z) = \mathcal{E}_0 \mathcal{H}_z(\rho, p_0) \frac{\operatorname{sgn}(z)}{\cos(k_0 p_0 L)} \cos[k_0 p_0(L - |z|)], \quad |z| < L. \quad (48)$$

Similarly, the azimuthal electric field is given by

$$E_\phi(\rho, z) = \mathcal{E}_0 \mathcal{E}_\phi(\rho, p_0) \frac{\operatorname{sgn}(z)}{\cos(k_0 p_0 L)} \cos[k_0 p_0(L - |z|)], \quad |z| < L. \quad (49)$$

Expressions (45), (46), (48), and (49) give the tangential (with respect to the cylindrical surface $\rho = \text{const}$) components of the field inside the dielectric sheath of a finite-length antenna.

The axial current of the antenna is found from (45) as $I(z) = 2\pi a_0 H_\phi(a_0, z)$. Therefore,

$$I(z) = \frac{I_0}{\sin(k_0 p_0 L)} \sin[k_0 p_0(L - |z|)], \quad |z| < L, \quad (50)$$

where I_0 is the current at the antenna input. In the case $k_0 p_0 L \ll 1$, we evidently have, from (50),

$$I(z) = I_0 \left(1 - \frac{|z|}{L} \right). \quad (51)$$

If $\tilde{\varepsilon} = 1$ and the current wavelength is determined by the sheath parameters, i.e., $p_0 \approx \tilde{\varepsilon}^{1/2} = 1$, then the inequality $k_0 p_0 L \ll 1$ reduces to $k_0 L \ll 1$, which is ensured for almost all dipole antennas operating in the whistler range under conditions of actual experiments in the laboratory plasma and space. It is important that the conditions for the applicability of a triangular current distribution in the form (51) can be satisfied if the antenna is not short compared to the maximum whistler wavelength $\lambda_W = 2\pi/(k_0 P_e)$ in the plasma, provided that $P_e \gg \tilde{\varepsilon}^{1/2}$. It is also worth mentioning that the circumferential current on a finite-length antenna can readily be found from (48) as $I_\phi(z) = -H_z(a_0, z)$.

The above results imply that the current distribution on a cylindrical antenna surrounded by a magnetoplasma and operating in the whistler range can be described using the transmission-line theory. Within the framework of such an approach, the quantity p_0 determining the current distribution along the single-wire line corresponding to the antenna is obtained from (22). We found that this quantity is the propagation constant of the eigenmode whose amplitude is constant along the wire, provided that dissipative losses are negligible. On the contrary, for antennas located in isotropic or uniaxially anisotropic media, the ‘‘propagation constant’’ determining the current distribution corresponds to the branch point of the integrand in the integral representation of the current on an infinite cylindrical conductor [6]. For the latter case, therefore, the magnitude of the current wave should decay with distance from the excitation point due to radiation losses.

4.2. Input Impedance of a Finite-Length Antenna

To determine the input impedance $Z = R + iX$ of a finite-length antenna with the known shape of the current distribution, standard techniques based on Poynting’s theorem can be used [9, 12, 25]. Then, knowing the antenna input impedance Z , the current I_0 at the antenna input is found as $I_0 = V/Z$. A very simple expression for the antenna reactance X can be obtained in the case of a moderately thick sheath (e.g., see Fig. 3) where

$$p_0 \approx \tilde{\varepsilon}^{1/2}, \quad \ln(1+s) \gg (\tilde{\varepsilon}/\varepsilon) \ln(\rho_*/a). \quad (52)$$

Here, $\rho_* = L|\varepsilon/\eta|^{1/2}$ for a “short” antenna ($k_0 p_0 L < 1$) and $\rho_* = (k_0 |\text{Im } q_{1,2}(p_0)|)^{-1}$ for a “long” antenna ($k_0 p_0 L > 1$). It is also assumed that the conditions used for the derivation of (31) continue to hold. Then almost all of the antenna near-zone field is localized in the sheath and the field penetrating into the surrounding magnetoplasma can be neglected. In this case, the antenna reactance is readily expressed via the difference of the time-averaged electric and magnetic energies stored inside the sheath (see [25] for details). Taking into account the approximate expressions

$$E_\rho \approx i \frac{Z_0}{k_0 \tilde{\varepsilon}} \frac{\partial H_\phi}{\partial z}, \quad H_\phi \approx \frac{I(z)}{2\pi\rho},$$

which are valid for the predominant field components inside the sheath, and using some general relationships given for the reactive part of the input impedance in [25], we arrive at the formula

$$X = -\frac{Z_0}{\pi \tilde{\varepsilon}^{1/2}} \ln \frac{a}{a_0} \cot k_0 p_0 L. \quad (53)$$

It should be mentioned that, in fact, the approximation yielding the last expression for X corresponds to the transmission-line theory for an insulated antenna located in a magnetoplasma. In the case $k_0 p_0 L \ll 1$, formula (53) takes the form

$$X = -\frac{Z_0}{\pi k_0 p_0 L \tilde{\varepsilon}^{1/2}} \ln \frac{a}{a_0}. \quad (54)$$

It is interesting to compare the reactance of an insulated antenna with that of a sheathless antenna. In the absence of the insulation, a simple universal formula for the reactance of a sheathless antenna of arbitrary length located in a magnetoplasma cannot be derived. For a thin ($a_0 \ll |\varepsilon/\eta|^{1/2} L$), short ($k_0 L \varepsilon^{1/2} \ll 1$) sheathless antenna, it is well known [1] that

$$X = -\frac{Z_0}{\pi k_0 L \varepsilon} \left[\ln \left(\sqrt{\frac{\varepsilon}{|\eta|}} \frac{L}{a_0} \right) - 1 \right]. \quad (55)$$

But if a thin sheathless antenna, for which the inequalities $k_0 a_0 \ll 1$ and $|\ln k_0 a_0| \gg |\ln q_{1,2}|$ hold, is very long such that $k_0 L \varepsilon^{1/2} \gg 1$, then

$$X = -\frac{Z_0}{\pi \varepsilon^{1/2}} \gamma \ln \frac{1}{k_0 a_0} \cot k_0 L \varepsilon^{1/2}, \quad (56)$$

where γ is a factor of order unity. According to numerical calculations, $\gamma \simeq 0.59$ in the whistler range. Formula (56) can be derived using the results of [17].

By comparing (53) with (55) and (56), it is seen that the reactance X in the presence of the insulating sheath can differ significantly from that for a sheathless antenna. In the case where the antenna comprises the ion sheath, the reactance can evidently be changed by varying the sheath thickness. For instance, the sheath effects can be almost avoided if the antenna static potential is ensured to be close to that of the surrounding plasma [9]. This can be provided by the application of an appropriate static voltage between the antenna and the other comparatively large conducting object immersed in the plasma. On the contrary, when the ion sheath effects are well pronounced, the antenna is expected not to be coupled strongly to the plasma. Hence, the reactive part of the input impedance will tend to that described by (53). For an actual antenna in a magnetoplasma, the reactance may be somewhere between the quantity (53) and the quantity found in the absence of the ion sheath. Therefore, varying the antenna static potential, one can modify the antenna impedance, which may presumably be used for both diagnostic purposes and controlling the antenna characteristics.

To evaluate the resistive part R of the input impedance, we should calculate the power P_{rad} radiated from the antenna with the current distribution (50) and then use the relation $R = 2P_{\text{rad}}/|I_0|^2$. The total radiation power of the finite-length insulating antenna can be determined with the help of Huygens' principle. Since the fields $\vec{E}(\rho, z)$ and $\vec{H}(\rho, z)$ in the near zone of the antenna are known, fictitious electric and magnetic currents with the densities \vec{J}^e and \vec{J}^m , respectively, can be specified on the cylindrical surface $\rho = a$ for $|z| < L$. The quantities \vec{J}^e and \vec{J}^m are given by

$$\vec{J}^e(\vec{r}) = \hat{\rho}_0 \times \vec{H}(a, z) \delta(\rho - a), \quad \vec{J}^m(\vec{r}) = -\hat{\rho}_0 \times \vec{E}(a, z) \delta(\rho - a), \\ |z| < L. \quad (57)$$

According to Huygens' principle, the power radiated from the insulated antenna coincides with that radiated from the currents $\vec{J}^{e,m}$ into the surrounding medium:

$$P_{\text{rad}} = -\frac{1}{2} \text{Re} \int \left[\left(\vec{J}^e(\vec{r}) \right)^* \cdot \vec{E}(\vec{r}) + \left(\vec{J}^m(\vec{r}) \right)^* \cdot \vec{H}(\vec{r}) \right] d\vec{r}, \quad (58)$$

where $\vec{E}(\vec{r})$ and $\vec{H}(\vec{r})$ are the electric and magnetic fields excited by currents (57) in a homogeneous unbounded magnetoplasma whose parameters are identical to those of the plasma surrounding the antenna. Introducing the spatial Fourier transform of any function

$f(\vec{r})$ and its inverse as

$$f(\vec{n}) = \int f(\vec{r}) \exp(ik_0 \vec{n} \cdot \vec{r}) d\vec{r},$$

$$f(\vec{r}) = \frac{k_0^3}{(2\pi)^3} \int f(\vec{n}) \exp(-ik_0 \vec{n} \cdot \vec{r}) d\vec{n}$$

and using Parseval's theorem, we can express the radiated power (58) via the integral in \vec{n} -space:

$$P_{\text{rad}} = -\frac{k_0^3}{16\pi^3} \text{Re} \int \left[\left(\vec{\mathcal{J}}^e(\vec{n}) \right)^* \cdot \vec{E}(\vec{n}) + \left(\vec{\mathcal{J}}^m(\vec{n}) \right)^* \cdot \vec{H}(\vec{n}) \right] d\vec{n}. \quad (59)$$

Then we should perform integrations over n_z and the azimuthal angle $\chi = \tan^{-1}(n_y/n_x)$ in \vec{n} -space. These two integrations, whose details are described in [22], yield the radiated power in the form of an integral over $q = (n_x^2 + n_y^2)^{1/2}$. The resulting expression for P_{rad} turns out to be extremely cumbersome and will not be given here. A close inspection of P_{rad} shows that for the above-discussed parameter values, the power radiated from the antenna in the resonant part of the whistler range can be found, to a good approximation, by putting $\vec{\mathcal{J}}^e(\vec{r}) = \vec{J}(\vec{r})$ and $\vec{\mathcal{J}}^m(\vec{r}) = 0$ in (58) and neglecting the contribution from the azimuthal component of $\vec{J}(\vec{r})$ to P_{rad} . In particular, such an approximation is always applicable for the antenna in a magnetoplasma modeled upon the Earth's ionosphere if $\tilde{\varepsilon}$ is of order unity and the sheath thickness Δa is of the order of the Debye length or smaller. Taking into account formula (50) for the distribution of the axial current along z and performing the above-described integrations it follows from (59) that

$$R = Z_0 \frac{p_0^2}{\sin^2(k_0 p_0 L)} \frac{4}{\pi(-\eta)} \times \int_0^\infty \frac{q^2 + p_e^2(q) - \varepsilon}{q^2 - \eta} \frac{q^3 p_e(q) J_0^2(k_0 a_0 q)}{[q^4(1 - \varepsilon/\eta)^2 - 4q^2 g^2/\eta + 4g^2]^{1/2}} \times \frac{\sin^2[k_0 L(p_e(q) - p_0)/2] \sin^2[k_0 L(p_e(q) + p_0)/2]}{[p_e^2(q) - p_0^2]^2} dq, \quad (60)$$

where

$$p_e(q) = \left\{ \varepsilon - \frac{1}{2} \left(1 + \frac{\varepsilon}{\eta} \right) q^2 + \left[\frac{1}{4} \left(1 - \frac{\varepsilon}{\eta} \right)^2 q^4 - \frac{g^2}{\eta} q^2 + g^2 \right]^{1/2} \right\}^{1/2}.$$

Note that the function $p = p_e(q)$ describes the dependence of the axial wavenumber p of the whistler mode on the transverse wavenumber q (see Fig. 2 and [22]).

Since the eigenmode guided along the antenna is transversely localized, the quantity (60) calculated for the current (50) vanishes in the limit $L \rightarrow \infty$. Therefore, in the case $k_0 p_0 L \gg 1$, the contribution due to continuous-spectrum waves should be taken into account in the antenna current to determine correctly the resistive part of the input impedance. Allowance for this contribution can be important only near the excitation point $z = 0$ and the antenna ends $z = \pm L$. However, if the antenna length does not exceed several wavelengths of the eigenmode, then formula (50) for the antenna current can be safely used for evaluating R .

It follows from (53) and (60) that the input impedance is infinite if $k_0 p_0 L = \pi n$, i.e., $L = \lambda n/2$, where $n = 1, 2, \dots$. This is related to the fact that the approximate formula (50) was used for the antenna current. Therefore, the results of the transmission-line theory should be refined for this particular case. In this paper, we do not consider the corresponding corrections to the transmission-line theory since for most insulated antennas encountered in actual practice, the condition $L < \lambda/2$ usually holds in the whistler range.

Let us discuss some special cases in which the expression for R becomes simpler. In the case $k_0 p_0 L \ll 1$, when the current distribution is triangular, formula (60) reduces to

$$R = Z_0 \frac{4}{\pi(k_0 L)^2(-\eta)} \times \int_0^\infty \frac{q^2 + p_e^2(q) - \varepsilon}{q^2 - \eta} \frac{q^3}{p_e^3(q)} \frac{J_0^2(k_0 a_0 q) \sin^4(k_0 L p_e(q)/2)}{[q^4(1 - \varepsilon/\eta)^2 - 4q^2 g^2/\eta + 4g^2]^{1/2}} dq. \quad (61)$$

When $k_0 L \varepsilon^{1/2} \ll 1$, most contributions to the integral in (61) come from the region $|\eta|^{1/2} < q < |\eta|^{1/2}(k_0 L \varepsilon^{1/2})^{-1}$. For $q > |\eta|^{1/2}$, we can write

$$p_e(q) \simeq (-\varepsilon/\eta)^{1/2} q \operatorname{sgn} \varepsilon, \quad (q^2 + p_e^2(q) - \varepsilon)/(q^2 - \eta) \simeq 1 - \varepsilon/\eta.$$

In addition, we assume that $a_0 \ll |\varepsilon/\eta|^{1/2} L$. Then the integrand in (61) is greatly simplified, such that

$$R = Z_0 \frac{4}{\pi(k_0 L)^2} \frac{|\eta|^{1/2}}{\varepsilon^{3/2}} \int_0^\infty \frac{1}{q^2} \sin^4\left(\frac{k_0 L}{2} \frac{\varepsilon^{1/2}}{|\eta|^{1/2}} q\right) dq. \quad (62)$$

Evaluating the integral on the right-hand side of (62), we arrive at the expression

$$R = Z_0/(2k_0 L \varepsilon). \quad (63)$$

Note that (63) is precisely the result yielded by the quasi-static theory for an uninsulated antenna with a triangular current distribution [1].

We have thus established the conditions under which the quasi-static theory can be used for calculating the resistive part of the input impedance of a cylindrical insulated antenna in a resonant magnetoplasma. It should also be kept in mind that in the presence of the ion sheath, allowance for a sheath conductance can be important for correctly determining the resistive part of the antenna impedance at frequencies much lower than the ion plasma frequency [9]. When required, an appropriate correction term to R may be found using the approach described in [9].

5. CONCLUSIONS

In this paper, we have studied the current distribution and the input impedance of a perfectly conducting cylindrical antenna insulated from the surrounding magnetoplasma by a coaxial dielectric or free-space sheath and aligned with an external magnetic field. Main attention has been paid to analysis of the case where the antenna current is excited by a delta-function voltage source in the whistler frequency range. We have found that the current distribution on a rather thin, infinitely long antenna is determined by the contribution of the eigenmode guided along the antenna. It has been shown that the presence of the very thin insulating sheath around the antenna can lead to a decrease in the relative contribution of continuous-spectrum waves to the total current as compared with the case of a sheathless antenna. The propagation constant of the eigenmode was shown to depend significantly on the dielectric permittivity and thickness of the sheath.

Based on these results, a generalized transmission-line theory was developed for finding the characteristics of a finite-length antenna located in a resonant magnetoplasma. Within the framework of this theory, the current distribution is constructed, in a first approximation, as the standing current wave. In this case, the propagation constant of the eigenmode guided by the corresponding infinitely long antenna should be taken as the propagation constant of the current wave. Using the developed approach, we analyzed the current distribution of a finite-length antenna and proposed a method for calculating its input impedance. It follows from the results obtained that in the presence of the insulation, the short-antenna current approximation (see (51)) is applicable for an antenna which physically can be much longer than an uninsulated antenna, provided the condition $\tilde{\varepsilon} \ll \varepsilon$ is satisfied. Also, a possibility of varying the antenna characteristics by controlling the parameters of the ion sheath around the antenna wire was pointed out. This can be available by means of changing the static potential of the antenna with respect to that of the surrounding plasma. In particular,

for moderate thicknesses of the insulation, the antenna reactance can be made less dependent on the parameters of the surrounding plasma medium.

ACKNOWLEDGMENT

This work was supported by the European Commission and the General Secretariat of Research and Technology of Greece (project ENTER 01ER63) and in part by the Russian Foundation for Basic Research (project Nos. 04-02-16344a and 04-02-16506a), the Ministry of Education and Science of the Russian Federation (project Nos. 40.020.1.1.1171 and UR.01.01.024), and the Program for the State Support of the Leading Scientific Schools of the Russian Federation (project No. NSh-1639.2003.2).

REFERENCES

1. Balmain, K. G., "The impedance of a short dipole antenna in a magnetoplasma," *IEEE Trans. Antennas Propagat.*, Vol. AP-12, No. 5, 605-617, 1964.
2. Seshadri, S. R., "Radiation resistance of elementary electric-current sources in a magnetoionic medium," *Proc. IEE*, Vol. 112, No. 10, 1856-1868, 1965.
3. Wang, T. N. C. and T. F. Bell, "Radiation resistance of a short dipole immersed in a cold magnetoionic medium," *Radio Sci.*, Vol. 4, No. 2, 167-177, 1969.
4. Wang, T. N. C. and T. F. Bell, "On VLF radiation resistance of an electric dipole in a cold magnetoplasma," *Radio Sci.*, Vol. 5, No. 3, 605-610, 1970.
5. Hurd, R. A., "The admittance of a linear antenna in a uniaxial medium," *Can. J. Phys.*, Vol. 43, No. 6, 2276-2309, 1965.
6. Lee, S. W., "Cylindrical antenna in uniaxial resonant plasmas," *Radio Sci.*, Vol. 4, No. 2, 179-189, 1969.
7. Chugunov, Yu. V., "On the theory of a thin metal antenna in anisotropic media," *Izv. Vyssh. Uchebn. Zaved., Radiofiz.*, Vol. 12, No. 6, 830-834, 1969.
8. Chen, C. L. and S. R. Seshadri, "Infinite insulated cylindrical antenna in a simple anisotropic medium," *IEEE Trans. Antennas Propagat.*, Vol. AP-14, No. 6, 715-726, 1966.
9. Mareev, E. A. and Yu. V. Chugunov, *Antennas in Plasmas* [in Russian], Inst. Appl. Phys. Press, Nizhny Novgorod, 1991.

10. Lu, H.S. and K.K.Meï, "Cylindrical antennas in gyrotropic media," *IEEE Trans. Antennas Propagat.*, Vol. AP-19, No. 5, 669–674, 1971.
11. Eremin, S.M., "The impedance of an electric dipole in an anisotropic plasma," *Radiotekh. Élektron.*, Vol. 33, No. 9, 1852–1861, 1988.
12. King, R. W. P. and G. S. Smith, *Antennas in Matter: Fundamentals, Theory, and Applications*, MIT Press, Cambridge, Mass., 1981.
13. Adachi, S., T. Ishizone, and Y. Mushiaké, "Transmission line theory of antenna impedance in a magnetoplasma," *Radio Sci.*, Vol. 12, No. 1, 23–31, 1977.
14. Lee, S. W. and Y. T. Lo, "Current distribution and input admittance of an infinite cylindrical antenna in anisotropic plasma," *IEEE Trans. Antennas Propagat.*, Vol. AP-15, No. 2, 244–252, 1967.
15. Seshadri, S. R., "Input admittance of a cylindrical antenna in a magnetoionic medium," *J. Appl. Phys.*, Vol. 39, No. 5, 2407–2412, 1968.
16. Bhat, B., "Current distribution on an infinite tubular antenna immersed in a cold collisional magnetoplasma," *Radio Sci.*, Vol. 8, No. 5, 483–492, 1973.
17. Zaboronkova, T. M., A. V. Kudrin, and E. Yu. Petrov, "Current distribution on a cylindrical VLF antenna in a magnetoplasma," *Radiophys. Quantum Electron.*, Vol. 42, No. 8, 660–673, 1999.
18. Mushiaké, Y., "Electromagnetic waves along an infinitely long and thin conducting wire in a magneto-ionic medium," *J. Res. Natl. Bur. Stand.*, Vol. 69D, No. 4, 503–510, 1965.
19. Seshadri, S. R., "Guided waves on a perfectly conducting infinite cylinder in a magnetoionic medium," *Proc. IEE*, Vol. 112, No. 8, 1497–1500, 1965.
20. James, H. G. and K. G. Balmain, "Guided electromagnetic waves observed on a conducting ionospheric tether," *Radio Sci.*, Vol. 36, No. 6, 1631–1644, 2001.
21. Ginzburg, V. L., *The Propagation of Electromagnetic Waves in Plasmas*, 2nd ed., Pergamon Press, Oxford, 1970.
22. Kondrat'ev, I. G., A. V. Kudrin, and T. M. Zaboronkova, *Electrodynamics of Density Ducts in Magnetized Plasmas*, Gordon and Breach, Amsterdam, 1999.
23. Abramowitz, M. and I. A. Stegun (eds.), *Handbook of Mathematical Functions*, Dover, New York, 1970.

24. Azarenkov, N. A., I. B. Denisenko, and K. N. Ostrikov, "Wave properties of a cylindrical antenna immersed in a magneto-active plasma," *J. Plasma Phys.*, Vol. 50, Pt. 3, 369–384, 1993.
25. Jackson, J. D., *Classical Electrodynamics*, 3rd ed., John Wiley & Sons, New York, 1999.

Alexander V. Kudrin was born in Shadrinsk, Kurgan region, Russia, on March 27, 1965. He received the Ph.D. and D.Sc. degrees in radiophysics from the University of Nizhny Novgorod, Nizhny Novgorod, Russia, in 1994 and 2004, respectively. Since 1987, he has been with the Department of Radiophysics, University of Nizhny Novgorod, where he is currently an Associate Professor. He has also served as a Deputy Head of the Electrodynamics Division at Department of Radiophysics since 1996, and became a Deputy Head of Department of Radiophysics, University of Nizhny Novgorod, in 2004. He was a visiting scientist at the Democritus University of Thrace, Xanthi, Greece, in 2004. He has published more than 120 journal articles and conference papers and coauthored one book. His primary research interests include open waveguides in anisotropic media, antenna theory and wave propagation in plasmas, and nonlinear interactions between electromagnetic fields and plasmas.

Evgeny Yu. Petrov was born in Nizhny Novgorod, Russia, on March 14, 1975. He received the B.Sc. and M.Sc. degrees in physics and the Ph.D. degree in radiophysics from the University of Nizhny Novgorod, Nizhny Novgorod, Russia, in 1996, 1998, and 2001, respectively. Since 2001, he has been at the Department of Radiophysics, University of Nizhny Novgorod, where he is now a Senior Lecturer. In 2002, he received the URSI Young Scientist Award at the XXVIIth General Assembly of the International Union of Radio Science (URSI), Maastricht, The Netherlands. His current research deals with antenna theory and wave propagation in plasmas.

George A. Kyriacou was born in Famagusta, Cyprus, on March 25, 1959. He received the Electrical Engineering Diploma and the Ph.D. degree, both with honors, from the Democritus University of Thrace, Xanthi, Greece, in 1984 and 1988, respectively. Since January 1990, he has been with the Department of Electrical and Computer Engineering, Democritus University of Thrace, where he is currently an Associate Professor. He is the author of over 105 journal articles and conference papers. His main research interests include microwave engineering, open waveguides and antennas in anisotropic media,

applied electromagnetics, and biomedical engineering. Dr. Kyriacou is a member of IEEE and the Technical Chamber of Greece.

Tatyana M. Zaboronkova graduated from the University of Nizhny Novgorod, Nizhny Novgorod, Russia, in 1970. She received the Ph.D. degree from the University of Nizhny Novgorod in 1979, and the D.Sc. degree from the Radiophysical Research Institute, Nizhny Novgorod, in 1994. Since 1970, she has been with the Radiophysical Research Institute, Nizhny Novgorod, and since 1985, with the Technical University of Nizhny Novgorod, where she is currently a Professor at the Department of Applied Physics. She is the author or coauthor of one book and over 150 journal articles and conference papers. Her main research interests are in plasma physics, antenna theory, and the nonlinear theory of diffraction of electromagnetic waves.